

RSC Advances

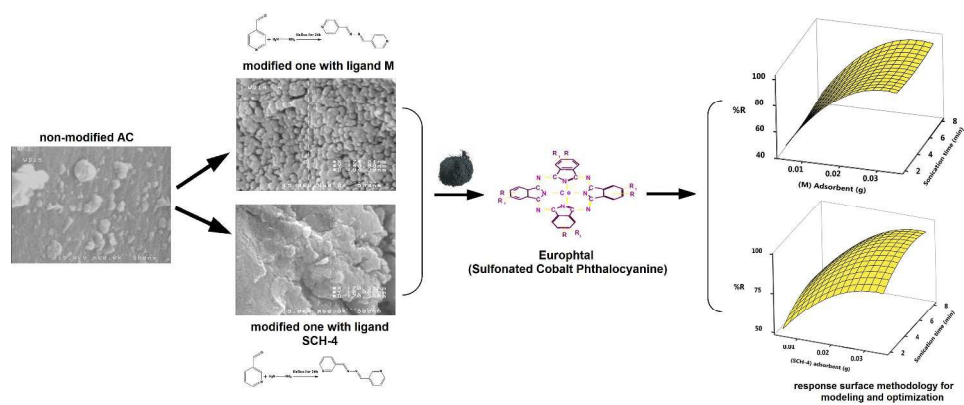


This is an *Accepted Manuscript*, which has been through the Royal Society of Chemistry peer review process and has been accepted for publication.

Accepted Manuscripts are published online shortly after acceptance, before technical editing, formatting and proof reading. Using this free service, authors can make their results available to the community, in citable form, before we publish the edited article. This *Accepted Manuscript* will be replaced by the edited, formatted and paginated article as soon as this is available.

You can find more information about *Accepted Manuscripts* in the [Information for Authors](#).

Please note that technical editing may introduce minor changes to the text and/or graphics, which may alter content. The journal's standard [Terms & Conditions](#) and the [Ethical guidelines](#) still apply. In no event shall the Royal Society of Chemistry be held responsible for any errors or omissions in this *Accepted Manuscript* or any consequences arising from the use of any information it contains.



1074x448mm (96 x 96 DPI)

Efficient adsorption of Europhtal onto activated carbon modified with ligands (1E, 2E)-1,2-bis (pyridin-4-ylmethylene) hydrazine (M) and (1E, 2E)-1,2-bis (pyridin-3-ylmethylene) hydrazine (SCH-4); Response surface methodology

M. Ghaedi^{*a}, E. Alam barkat^b, A. Asfaram^a, B. Mirtamizdoust^c, A.A. Bazrafshan^a, S. Hajati^{*d}

^a Chemistry Department, Yasouj University, Yasouj 75918-74831, Iran.

^b Chemistry Department, Islamic Azad University, Fars Science and Research Branch, Fars, Iran.

^c Department of Chemistry, Faculty of Science, University of Qom, 37185-359 Iran.

^d Department of Physics, Yasouj University, Yasouj 75918-74831, Iran.

*Corresponding authors at: Chemistry Department, Yasouj University, Yasouj 75918-74831, Iran, Tel/Fax: +98 741 2223048.

E-mail address: m_ghaedi@mail.yu.ac.ir; m_ghaedi@yahoo.com (M. Ghaedi); and at: Department of Physics, Yasouj University, Yasouj 75918-74831, Iran. Tel/Fax: +98 741 2223048;

E-mail address: hajati@mail.yu.ac.ir; (S. Hajati).

Abstract

Porous activated carbon was modified with (1E, 2E)-1, 2-bis (pyridin-4-ylmethylene) hydrazine (M) and (1E, 2E)-1, 2-bis (pyridin-3-ylmethylene) hydrazine (SCH-4). Characterization was performed using different techniques such as SEM, FTIR and ^1H NMR analysis. Then, these new adsorbents were used for efficient removal of Europhtal (Sulfonated Cobalt Phthalocyanine). Response surface methodology (RSM) was used to achieve operational conditions for efficient removal of Europhtal using activated carbon modified with novel ligands. To investigate the individual effect of variables involved and the effect of their possible interactions on the adsorption process, several systematic experiments were designed by varying the variables such as pH, sonication time, adsorbent dosage and dye concentration in the range of 2.0-11, 2-8 min, 0.005-0.035 g and 4–30 mg L^{-1} , respectively. The optimum values of pH, sonication time, adsorbent dosage and Europhtal concentration were found to be 7, 2 min, 30 mg L^{-1} and 0.03 g for the case modified with M and 7, 5 min, 30 mg L^{-1} and 0.03 g for one with SCH-4at which, the removal percentages were more than 98%. Adsorption equilibrium data were well fitted to Freundlich model with maximum adsorption capacities of 56.69 and 17.84 mg g^{-1} for M and SCH-4, respectively. The study of adsorption kinetics indicated that the dye uptake process follows the pseudo second-order and saturation type rate expressions for each Ligand.

Keywords: Europhtal; Response surface methodology; (1E, 2E)-1,2-bis (pyridin-4-ylmethylene) hydrazine (M); (1E, 2E)-1,2-bis (pyridin-3-ylmethylene) hydrazine

1. Introduction

The effluents composed of synthetic dyes arrive from different sources to the environment. Dyes are widely utilized in various industrial activities such as coloring, paper, textiles, cosmetics and food¹⁻³. Their complex (aromatic) molecular structures cause increase in their resistance to heat, oxidizing agent and biodegradation. Most dyes are toxic and harmful to some microorganisms and prevent from their catalytic activity⁴. The toxicity of dyes on plant, animal and human health is not well-known^{5, 6}. Several versatile approaches including ion exchange, photo-oxidation processes, flocculation, precipitation, microbiological decomposition and ozonation are applied for wastewater treatment and water quality enhancement. Low cost and easy-to-prepare adsorbents are the best for wastewater treatment and pollutants removal via the adsorption process⁷⁻¹⁴. The adsorption process provides an attractive alternative for water treatment, while is easy to handle, requires less maintenance and produce smaller amounts of sludge^{5, 15-17}. Most of adsorbents have high abundance and cheap, while have drawbacks such as poor mechanical and heat resistance and relatively limited adsorption capacity for dyes¹⁸⁻²⁰. Thus modification of adsorbents and improvement of their properties viz. reactive centers and surface area is a great demand. A catalyst solution comprising 30% of sulphonated cobalt phthalocyanine (Europhthal under the name 802) is generally used to remove mercaptan from hydrocarbon based on either its solution or liquid catalyst loaded on activated carbon. This catalyst is extensively applied in numerous refineries worldwide and it is necessary to develop novel materials and methods for its removal from various media. In this regard, development and search for novel adsorbent, especially nanoscale adsorbents are good choice to improve the characteristic performance of removal procedure. Huge number of reactive centers and sites on the surface of nanomaterials make them suitable for trapping other species. Activated carbon-based adsorbents

with unique porous reactive sites in the presence of versatile reaction centers like hydroxide, carboxylic and amide groups are good materials for subsequent modification through hydrogen bonding, π - π bonding and electrostatic reactions. Various organic reagents and chelating agents can be used for the modification on the surface of such adsorbents leading to more improvement in removal process performances.

The present work focuses on the synthesis of (1E, 2E)-1, 2-bis (pyridin-4-ylmethylene) hydrazine (M) and (1E, 2E)-1, 2-bis (pyridin-3-ylmethylene) hydrazine (SCH-4) as well as on their subsequent loading on AC followed by the characterization by SEM, FTIR and ^1H NMR. Then, the potential feasibility of M- and SCH-4- loaded AC for the Europhtal removal (as response) was investigated and the influences of various variables on the response were investigated and optimized. Statistical analysis was applied on the experimental data and results to make a predictive model and test the validity. The kinetic and equilibrium data were analyzed to understand the adsorption mechanism by applying different models to fit the experimental data.

2. Materials and methods

2.1. Materials and instruments

The Europhtal (Table 1) was purchased from Sigma Aldrich and its stock solution (100 mgL^{-1}) was prepared in double distilled water. Europhtal concentration was determined by measuring and analyzing the absorbance spectra before and after each experiment by a 2800-DR (UV-Vis) spectrophotometer at 664 nm. An ultrasonic bath with heating system (Bandelin sonorex) at frequency 40 kHz with power of 130 W was used for the ultrasound-assisted adsorption procedure. For pH measurements a Metrohm pH meter model-780 was used. The morphology

and size distribution of the M- and SCH-4-loaded AC were observed by scanning electron microscopy (SEM; Hitachi S-4160) under an acceleration voltage of 15 kV. The FTIR spectra of all compounds were recorded by using a JASCO-FTIR-480 instrument in the range of 4000–400 cm^{-1} with KBr as disc.

2.2. *Ultrasound-assisted adsorption method*

A batch process was used to evaluate the performance of Europhtal adsorption onto M- and SCH-4-loaded AC in presence of ultrasound. Adsorption experiments were performed in a cylindrical glass vessel by adding 0.02 g of either of adsorbents into 50 mL of Europhtal solution at known concentration (4 and 30 mg L^{-1}) at pH 7 that optimized by CCD. The vessel was immersed in an ultrasonic bath for 2.8 min time at room temperature. After this time, solutions were analyzed for determining the final Europhtal concentration by using a UV–Vis spectrophotometer set at a wavelength of 664 nm. The experiments were also performed in the initial dye concentration range of 5–40 mg L^{-1} to obtain adsorption isotherms. The dye removal percentage (R %) was calculated using the following equation:

$$R\% = \frac{C_0 - C_t}{C_0} \times 100, \quad (1)$$

where C_0 and C_e (mg L^{-1}) are the initial and equilibrium dye concentrations in aqueous solution, respectively. Adsorbed dye amount (q_e (mg g^{-1})) was calculated by the following mass balance relationship:

$$q_e = \frac{(C_0 - C_e)V}{W}, \quad (2)$$

where, V (L) is the volume of the solution and W (g) is the mass of the adsorbent.

2.3. Preparation of AC from acorn

The seed shells correspond to approximately 25% of the whole acorn. In order to separate shell from seeds, about 2 kg of acorn was cooked in a 1.0 L glass beaker for 2 h. afterwards, the acorn seeds were immersed in 2 L of deionized water and heated to boil for two more hours in order to remove the water soluble phenolic compounds and to avoid from their releases during the adsorption experiments. Subsequently, the acorn wastes were washed with distilled water and dried at 70 °C in an air-supplied oven for 8 h and was grounded thereafter in a disk-mill and sieved (70–100 mesh) subsequently. Sieved mass were then performed carbonization process in argon atmosphere at the temperature increase rate of 5 °C/min to the final temperature of 500 °C and kept for 1 h. The mass was then cooled and washed thoroughly several times by distilled water and dried²¹.

2.4. Synthesis of (1E, 2E)-1,2-bis(pyridin-4-ylmethylene)hydrazine (M)

1 ml (11 mmol) of hydrazine was added dropwise to a solution of isonicotinaldehyde (2.35 mL, 22 mmol) dissolved in ethanol (15 mL). Two drops of acetic acid were added and the mixture was stirred at room temperature for 24 h. The yellow solid that formed (with yield=73%) was filtered and washed several times with ethanol/ether (1:1) (See Fig. 1a for synthesis procedure).

2.5. Synthesis of (1E,2E)-1,2-bis(pyridin-3-ylmethylene)hydrazine (SCH-4)

1 mL (11 mmol) of hydrazine was added dropwise to a solution of nicotinaldehyde (2.4 mL, 20 mmol) dissolved in ethanol (15 mL). Two drops of formic acid were added and the mixture was stirred at room temperature for 24 h. The product (with yield=73%) was filtered and washed in the same way as done for ligand M (See Fig. 1b for synthesis procedure).

2.6. Central composite design (CCD)

To reduce the number of experiments required, a standard CCD (with 31 experiments) under RSM was applied. It helped us to determine regression model equations and operating conditions at which the maximum R% (as response) is achieved²²⁻²⁴. Moreover, the advantage of this procedure is the possibility of finding the effects of interaction between each pair of the variables involved such as pH (x_1), sonication time (x_2), adsorbent dosage (x_3) and Europhtal concentration (x_4) on the response (R %) in addition to their individual effects. As mentioned above, two materials were used as adsorbent which are M- and SCH-4-loaded activated carbon. The ranges of variation were set as 2-11 for the pH, 2-8 min for the sonication time, 0.005-0.035 g for the adsorbent amount, and 4-30 mg L⁻¹ for the Europhtal concentration (See Tables 2 and 3). CCD has been discussed in detail in Refs.^{13, 19, 25}. In general, the following equation may be used to model the experimentally obtained response versus variables involved.

$$R\% = \beta_0 + \sum_{i=1}^4 \beta_i x_i + \sum_{i=1}^4 \beta_{ii} x_i^2 + \sum_{i=1}^4 \sum_{j=1}^4 \beta_{ij} x_i x_j \quad (3)$$

In this equation, β_0 , β_i , and β_{ii} are constant coefficients corresponding to zero-, first- and second-order terms, respectively. β_{ij} is the coefficient of interaction term. Depending on the extent to which each term plays a role this model may be varied.

2.7. Model fitting and statistical analysis

The CCD-based experimental data were analyzed, using Minitab software version 17.0, to be fitted to a second-order polynomial equation and then the regression coefficients were obtained. The analysis of variance (ANOVA) was performed to justify the significance and adequacy of the developed regression model. The adequacy of the model was also evaluated by calculating the determination coefficient (R^2) in addition to testing it for the lack of fit.

3. Results and discussion

3.1. Characterization of adsorbent

FTIR and ^1H NMR spectra of the ligand M were acquired and shown in Fig. 2. The FTIR absorption band at 1628 cm^{-1} of the Imine factor, $\nu_{\text{C}=\text{N}}$, confirms the formation of the Schiff-base ligand. Some important absorption bands of the ligands are given in Table 4 and in good agreement with what has been reported^{26,27}.

Fig. 3 shows the FTIR and ^1H NMR spectra of the ligand SCH-4. The absorption band appeared around the frequency 1625 cm^{-1} in the FTIR spectrum of the Ligand SCH-4, corresponds to $\nu_{\text{C}=\text{N}}$, confirming the formation of the Schiff-base ligand. Detailed absorption bands of this ligand are given in Table 4, consistent to that reported elsewhere²⁸.

The morphology of non-modified AC (Fig. 4(a)) and that of modified one with either ligand M (Fig. 4(b)) or SCH-4 (Fig. 4(c)) were characterized by SEM showing approximate particle

size in the range of 40-80 nm. The surface modification is clearly seen after the deposition of ligands onto AC (Figs. 4(b) and 4(c)).

3.2. Central composite design (CCD)

Total 31 experiments (runs) were designed by Minitab software version 17.0. The tests for significance of regression model for both responses were evaluated and the results of ANOVA tests are presented in Table 5. From ANOVA, the factors with p-values less than 0.05 were distinguished to be significant. The p-values (0.343 and 0.0554 for M and SCH-4 data, respectively) corresponding to the lack of fits for the models applied indicated non-significant lack of fit. However, the model for predicting R% of Europhtal corresponding to either M- or SCH-4-based adsorbent was reconstructed to filter out non-significant factors. Thus the predictive models were applied as follow:

$$R\%_{Europhtal} = 64.9 + 5.49x_1 + 2228x_3 - 2.416x_4 - 0.827x_1^2 - 71468x_3^2 + 179.7x_1x_3 + 69.7x_3x_4 \quad \text{for M-loaded AC,} \quad (4)$$

$$R\%_{Europhtal} = 114.3 + 0.25x_1 - 1.77x_2 + 1761x_3 - 5.92x_4 - 0.584x_1^2 - 0.686x_2^2 - 43475x_3^2 + 0.0322x_4^2 + 0.2195x_1x_4 + 0.491x_2x_4 + 36.4x_3x_4 \quad \text{for SCH-4-loaded AC,} \quad (5)$$

Positive and negative signs in each equation imply synergistic and antagonistic effect of the variables, respectively. The values of determination coefficient (R^2) were found to be 0.985 and 0.968 for the Europhtal removal percentage by using M- and SCH-4-loaded AC, respectively, confirming the good agreement between the experimental and predicted values.

3.3. Response surface methodology

The curvature natures of Fig. 5 and 6 show the response surface plots of removal (%) and confirm strong interaction among variables.

Fig 5(a) and 6(a) strongly supports that elevating the adsorbent amount and dye concentration lead to enhance in Europhtal removal percentage. The increase in the amount of dye concentration leads to decrease in its removal percentage. The low and high initial dye concentrations have opposite trend. The small ratio of solute concentrations to non-occupied reactive adsorbent sites cause acceleration of dye adsorption and subsequent increase in removal percentage, while saturation of adsorption sites is associated with reduce in removal percentage at higher amount of target compounds. The opposite correlation among initial Europhtal concentration, removal percentage and actual amount of adsorbed Europhtal clearly indicate the dependency of Europhtal adsorption to its initial concentration.

Fig. 5(b) shows the combined effect of adsorbent and pH on adsorption of Europhtal onto adsorbent at constant Europhtal initial concentration (30 mg L^{-1}). Raising pH leads to significant influence on removal percentage and at constant pH, removal percentage increases with raising the M value. The Europhtal removal decreases at lower amount of adsorbent and approximate constant trend was seen at higher amount of adsorbent.

The increase in amount of adsorbent leads to significant decrease in sonication time (Fig. 6b), while the removal percentage at fixed sonication time has positive correlation with amount of adsorbent.

Fig. 6(d) shows the interaction of pH with initial Europhtal concentration and their relation with removal percentage. The pH has positive correlation with removal percentage, while higher pH and lower adsorbent concentration led to achievement of lower removal percentage. At low initial pH, protonation of the adsorbent functional groups led to generation of positive charge and

appearance of the strong attractive forces between the Europhtal molecule and adsorbent surface (increase in removal percentage).

3.4. Optimization

The profile for desirable option with predicted values in the Minitab software was used for the optimization of the process (Fig. 7). The profile for desirable responses was chosen after specifying the DF for each dependent variable (removal percentage) by assigning predicted values. The scale in the range of 0.0 (undesirable) to 1.0 (very desirable) was used to obtain a global function (D) that its maximum (100%) value concern to Europhtal adsorption was achieved in this research.

Maximum removal (>98.8%) was obtained at optimum conditions set as: 2 min of time, 0.03 g of adsorbent, initial Europhtal concentration of 30 mg L⁻¹ at pH 7 by AC-M and 5 min of time, 0.03 g of adsorbent, initial Europhtal concentration of 30 mg L⁻¹ at pH 7 by AC-SCH-4. The validity of duplicate assenting experiments at the optimized value of all parameters was investigated. The results were closely correlated with the data obtained from optimization analysis using CCD.

3.5. Adsorption equilibrium study

Common isotherm models such as Langmuir, Freundlich, Temkin and Dubinin-Radushkevich (D-R) are generally applied to discuss the equilibrium characteristics of the adsorption process²⁹⁻³². The constant parameters of the isotherms equations for this adsorption process and their correlation coefficient (R^2) are summarized in Table 6. Based on the linear form of Langmuir isotherm model²⁹ (according to Table 6), the values of K_L (the Langmuir

adsorption constant ($L\ mg^{-1}$) and Q_{max} (theoretical maximum adsorption capacity ($mg\ g^{-1}$)) were obtained, respectively, from the intercept and slope of the plot of C_e/q_e vs C_e .

The parameters of Freundlich isotherm model³⁰ such as K_F and $1/n$ (the capacity and intensity of the adsorption) were calculated from the intercept and slope of the linear plot of $\ln q_e$ versus $\ln C_e$, respectively (See Table 6). The values of $1/n$ were found to be 0.283 and 0.3385 corresponding to M-AC and SCH-4-AC, respectively, which show the high tendency of the adsorbents for the adsorption of Europhtal. Furthermore, high R^2 values (0.992 and 0.994 for M-AC and SCH-4-AC, respectively) show the suitability of Freundlich isotherm model for fitting the experimental data over the whole concentration range.

The heat of adsorption and the adsorbent–adsorbate interaction were evaluated by using Temkin isotherm model³³. B is the Temkin constant related to heat of the adsorption ($J\ mol^{-1}$), T is the absolute temperature (K), R is the universal gas constant ($8.314\ J\ mol^{-1}\ K^{-1}$) and K_T is the equilibrium binding constant ($L\ mg^{-1}$). R^2 values obtained from applying this model are lower than that corresponding to the Freundlich and Langmuir model. Therefore, it is concluded that the Freundlich isotherm represents a better fit to experimental data than the Langmuir isotherm.

Another commonly used model to explain equilibrium data for the adsorption onto a surface in liquid phase is Dubinin-Radushkevich (D-R)³² which is used to estimate the porosity apparent free energy and the characteristics of adsorption. In the D–R isotherm, K ($mol^2\ (kJ^2)^{-1}$) is a constant related to the adsorption energy, Q_{max} ($mg\ g^{-1}$) is the theoretical saturation capacity, ϵ is the Polanyi potential. The slope of the plot of $\ln q_e$ versus ϵ^2 gives K and the intercept yields the Q_m value. The mean free energy of the adsorption (E) is known as the free energy change when one mole of ion is transferred from the solution to the surface of the sorbent is calculated. The value of correlation coefficient obtained from D-R model is much lower than that from other

isotherms mentioned above. This means that the D–R equation represents the poorer fit to the experimental data compared to other isotherm equations.

3.6. Kinetics study

In order to examine the mechanism of adsorption process such as mass transfer and chemical reaction, a suitable kinetic model is needed to analyze the rate data. Many models such as homogeneous surface diffusion model, pore diffusion model and heterogeneous diffusion model (also known as pore and diffusion model) have been extensively applied in batch reactors to describe the transport of adsorbates inside the adsorbent particles^{34, 35}. The kinetics of Europhtal adsorption onto M-AC and SCH-4-AC was assessed using different models such as pseudo-first-order³⁶, pseudo-second-order³⁷, intraparticle diffusion³⁸ and Elovich³⁹ models (See Table 7). Among these models the criterion for their applicability is based on the respective correlation coefficient (R^2) and agreement between experimental and calculated value of q_e . The high values of R^2 (~0.999) and good agreement between two q_e values obtained from applying pseudo-second-order kinetic model indicate that the adsorption of Europhtal on either of M-AC and SCH-4-AC follows this model (Table 7).

In this work we have chosen two long, rigid bipyridyl-based ligands, (1E, 2E)-1,2-bis (pyridin-4-ylmethylene) hydrazine and (1E, 2E)-1,2-bis (pyridin-3-ylmethylene) hydrazine to react with Cobalt Phthalocyanine. They are natural ligands with two suitable sites for chelating to metals. The “N” atoms in the aromatic rings (pyridyl groups) connect to metal centers. These ligands can link two metals (or metal groups)^{26, 27}. Schematic diagrams for adsorption of this catalyst on both new adsorbents were presented in Figs. 8, 9.

3.7. *Application to Real Samples*

In order to observe the efficiency of M-AC and SCH-4-AC for the removal of Europhtal dye from real effluents, three effluent streams were collected separately and the adsorption experiments were performed. Adsorption experiments were conducted using optimum conditions. More than 96% of dye removal was achieved for all the effluents (Table 8).

4. Conclusion

Activated carbon was modified with ligands (1E, 2E)-1,2-bis (pyridin-4 ylmethylene) hydrazine (M) and (1E,2E)-1,2-bis (pyridin-3-ylmethylene) hydrazine (SCH-4) and characterized using SEM, FTIR and ^1H NMR analysis. Very small amount of each adsorbent (0.03 g) was used for efficient adsorption of Europhtal assisted by ultrasonication. Statistical modeling of the experiments resulted in the prediction of optimal conditions at which very high percentage of Europhtal is rapidly removed within a couple of minutes. Different models were applied to study the isotherm and kinetics of adsorption process which respectively showed the applicability of Freundlich isotherm and pseudo-second-order kinetics for both adsorbents. The adsorption capacities of M-AC and SCH-4-AC were found to be 56.69 mg g^{-1} and 17.84 mg g^{-1} , respectively.

Acknowledgement

The authors express their appreciation to the Graduate School and Research Council of the Islamic Azad University, Fars Science and Research Branch for financial support of this work.

References

1. M. Ghaedi, S. Heidarpour, S. Nasiri Kokhdan, R. Sahraie, A. Daneshfar and B. Brazesh, *Powder. Technol.* 2012, **228**, 18-25.
2. F. A. Pavan, E. C. Lima, S. L. Dias and A. C. Mazzocato, *J. hazard. mater.* 2008, **150**, 703-712.
3. A. Asfaram, M. Ghaedi, S. Agarwal, I. Tyagi and V. Kumar Gupta, *RSC Adv.*, 2015, **5**, 18438-18450.
4. S. Arivoli, M. Hema, S. Parthasarathy and N. Manju, *J. Chem. Pharm. Res.*, 2010, **2**, 626-641.
5. M. Ghaedi, B. Sadeghian, A. A. Pebdani, R. Sahraei, A. Daneshfar and C. Duran, *Chem. Eng. J.* 2012, **187**, 133-141.
6. H. Lata, V. Garg and R. Gupta, *Dyes and pigments*, 2007, **74**, 653-658.
7. S. Hajati, M. Ghaedi, F. Karimi, B. Barazesh, R. Sahraei and A. Daneshfar, *J. Ind. Eng. Chem.* 2014, **20**, 564-571.
8. M. Ghaedi, M. Pakniat, Z. Mahmoudi, S. Hajati, R. Sahraei and A. Daneshfar, *Spectrochim. Acta Part A*, 2014, **123**, 402-409.
9. M. Fathi, A. Asfaram and A. Farhangi, *Spectrochim. Acta Part A*, 2015, **135**, 364-372.
10. S. Hajati, M. Ghaedi and S. Yaghoubi, *J. Ind. Eng. Chem.* 2015, **21**, 760-767.
11. V. Garg, R. Gupta and T. Juneja, *Chem. Biochem. Eng. Q.*, 2004, **18**, 417-422.
12. P. K. Malik, *Dyes and pigments*, 2003, **56**, 239-249.
13. M. Ghaedi, H. Mazaheri, S. Khodadoust, S. Hajati and M. K. Purkait, *Spectrochim. Acta Part A*, 2015, **135**, 479-490.
14. J. Fu, Z. Chen, M. Wang, S. Liu, J. Zhang, J. Zhang, R. Han and Q. Xu, *Chem. Eng. J.* 2015, **259**, 53-61.
15. J. P. Silva, S. Sousa, I. Gonçalves, J. J. Porter and S. Ferreira-Dias, *Sep. Purif. Technol.* 2004, **40**, 163-170.
16. N. K. Amin, *J. Hazard. Mater.* 2009, **165**, 52-62.
17. M. Ghaedi, S. Hajjati, Z. Mahmudi, I. Tyagi, S. Agarwal, A. Maity and V. Gupta, *Chem. Eng. J.* 2015, **268**, 28-37.

18. A. Baçaoui, A. Yaacoubi, A. Dahbi, C. Bennouna, R. P. T. Luu, F. Maldonado-Hodar, J. Rivera-Utrilla and C. Moreno-Castilla, *Carbon*, 2001, **39**, 425-432.
19. S. Hajati, M. Ghaedi and H. Mazaheri, *Desalination and Water Treatment*, 2014, 1-15.
20. R. Azargohar and A. Dalai, *Microporous and mesoporous materials*, 2005, **85**, 219-225.
21. M. Ghaedi, H. Hossainian, M. Montazerzohori, A. Shokrollahi, F. Shojaipour, M. Soylak and M. K. Purkait, *Desalination*, 2011, **281**, 226-233.
22. A. Asfaram, M. Ghaedi, S. Hajati, A. Goudarzi and A. A. Bazrafshan, *Spectrochim. Acta Part A*, 2015, **145**, 203-212.
23. M. Roosta, M. Ghaedi, A. Daneshfar, R. Sahraei and A. Asghari, *J. Ind. Eng. Chem.* 2015, **21**, 459-469.
24. M. Ghaedi, S. Khodadoust, H. Sadeghi, M. A. Khodadoust, R. Armand and A. Fatehi, *Spectrochim. Acta Part A*, 2015, **136**, 1069-1075.
25. M. Roosta, M. Ghaedi, A. Daneshfar, S. Darafarin, R. Sahraei and M. Purkait, *Ultrason. sonochem.* 2014, **21**, 1441-1450.
26. Y.-B. Dong, M. D. Smith, R. C. Layland and H.-C. zur Loye, *Chem. mater.* 2000, **12**, 1156-1161.
27. D. M. Ciurtin, Y.-B. Dong, M. D. Smith, T. Barclay and H.-C. zur Loye, *Inorg. chem.* 2001, **40**, 2825-2834.
28. D.-Q. Li, X. Liu and J. Zhou, *Inorg. Chem. Communic.* 2008, **11**, 367-371.
29. I. Langmuir, *J. Am. Chem. Soc.* 1916, **38**, 2221-2295.
30. H. Freundlich, *Z Physics Chemistry*, 1906, **57**, 385-471.
31. M. Temkin and V. Pyzhev, 1940.
32. M. Dubinin and L. Radushkevich, *Chem. Zentr*, 1947, **1**, 875-889.
33. M. Temkin and V. Pyzhev, *Acta physiochim. URSS*, 1940, **12**, 217-222.
34. M. Ghaedi, A. Ansari, M. Habibi and A. Asghari, *J. Ind. Eng. Chem.* 2014, **20**, 17-28.
35. I. D. Mall, V. C. Srivastava, N. K. Agarwal and I. M. Mishra, *Colloid. and Surfaces A: Physicochemical and Engineering Aspects*, 2005, **264**, 17-28.
36. S. Lagergren, *Kungliga Svenska Vetenskapsakademiens Handlingar*, 1898, **24**, 1-39.

37. Y.-S. Ho and G. McKay, *Process Biochemistry*, 1999, **34**, 451-465.
38. H. A. AL-Aoh, R. Yahya, M. Jamil Maah and M. Radzi Bin Abas, *Desalination and Water Treatment*, 2013, 1-13.
39. S. Kaur, S. Rani, R. Mahajan, M. Asif and V. K. Gupta, *J. Ind. Eng. Chem.* 2014.

Figure captions:

Fig. 1 Procedure for the synthesis of **a**) (1E, 2E)-1, 2-bis (pyridin-4-ylmethylene) hydrazine. **b**) (1E, 2E)-1, 2-bis (pyridin-3-ylmethylene) hydrazine.

Fig. 2. FT-IR and ^1H NMR spectrum of the ligand (1E, 2E)-1, 2-bis (pyridin-4ylmethylene) hydrazine (M)

Fig. 3. FT-IR and ^1H NMR spectrum of the ligand (1E, 2E)-1, 2-bis (pyridin-3-ylmethylene) hydrazine (SCH-4)

Fig. 4. SEM of AC **(a)** Non-modified **(b)** modified by (1E, 2E)-1, 2-bis (pyridin-4-ylmethylene) hydrazine (M) **(c)** modified by (1E, 2E)-1, 2-bis (pyridin-3-ylmethylene) hydrazine (SCH-4).

Fig. 5. Response surfaces for the Europhtal removal by M-loaded AC: (a) X_1 - X_3 and (b) X_3 - X_4

Fig. 6. Response surfaces for the Europhtal removal by SCH-4-loaded AC: (a) X_1 - X_4 ; (b) X_2 - X_4 and (c) X_3 - X_4 .

Fig. 7. Profiles for predicated values and desirability function for removal percentage of Europhtal by ligands M and SCH-4. Dashed line indicated current values after optimization.

Fig. 8. Reaction between (1E, 2E)-1, 2-bis (pyridin-4-ylmethylene) hydrazine and Cobalt Phthalocyanine

Fig. 9. Reaction between (1E, 2E)-1, 2-bis (pyridin-3-ylmethylene) hydrazine and Cobalt Phthalocyanine

Table 1: Properties of the Europhtal dye

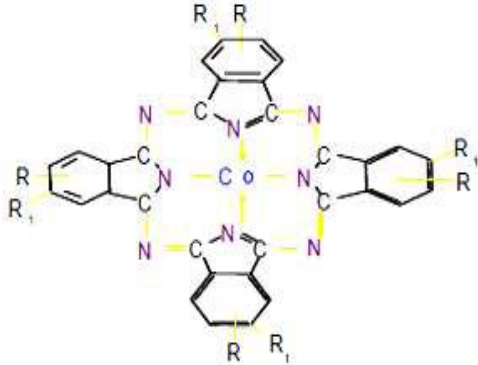
Product Identification	
Trade Name	Europhtal Additive 802
Appearance	Blue Liquid Solution
Chemical Name or generic name	Sulfonated Cobalt Phthalocyanine (Sodium salt)
Molecular Structure	 <p>R: -SO₃H⁻, Cl⁻, OH⁻, Br⁻ R₁: PhCH₂⁻, NO₂⁻, NH₂⁻</p>
Chemical Formula	C ₃₂ H _{16-i} N ₈ Co(SO ₃ Na) _i
CAS Number	90294-83-0
EINECS Number	290-971-9
shelf life	Not limited when stored in normal conditions: (temperature: 5 to 40 °C; relative humidity: less than 90 %)
Maximum wavelength (λ _{max}), nm	664 nm
USES	Desulphuration Catalyst for oils
Physical state	Liquid
Colour:	Blue
pH:	7.0 to 9.0
Decomposition temperature	> 300°
Relative density (Water)	1,15
Solubility	Soluble in water
Acute toxicity	LD 50> 2000 mg/kg (oral rat).
Hazardous reaction with	None under normal conditions of use.

Table 2
Factors in CCD and their levels.

Factors	Levels				
	Low (-1)	Central (0)	High (+1)	- α	+ α
X ₁ : pH	4.25	6.5	8.75	2	11
X ₂ : Sonication time (min)	3.5	5	6.5	2	8
X ₃ : Adsorbent (g)	0.0125	0.02	0.0275	0.005	0.035
X ₄ : dye concentration (mg L ⁻¹)	10.5	17	23.5	4	30

Table 3. Experimental runs and responses

Run	X ₁	X ₂	X ₃	X ₄	M	SCH-4
					Europhtal R%	Europhtal R%
1	8.75	3.5	0.0125	10.5	70.059	73.548
2	8.75	3.5	0.0125	23.5	56.111	62.209
3	4.25	6.5	0.0275	23.5	87.209	95.312
4	4.25	3.5	0.0275	10.5	94.230	94.820
5	8.75	6.5	0.0125	10.5	76.219	64.400
6	6.50	8.0	0.0200	17.0	92.277	90.079
7	11.0	5.0	0.0200	17.0	64.070	70.370
8	4.25	3.5	0.0275	23.5	90.285	86.140
9(C)	6.50	5.0	0.0200	17.0	90.079	91.320
10	2.00	5.0	0.0200	17.0	78.930	84.830
11	6.50	2.0	0.0200	17.0	88.537	76.404
12	8.75	3.5	0.0275	23.5	93.181	88.251
13	8.75	3.5	0.0275	10.5	95.977	92.215
14	6.50	5.0	0.0050	17.0	48.863	65.640
15(C)	6.50	5.0	0.0200	17.0	89.030	90.706
16	6.50	5.0	0.0350	17.0	95.454	93.632
17	4.25	6.5	0.0125	23.5	65.934	72.012
18	8.75	6.5	0.0125	23.5	52.189	82.954
19	6.50	5.0	0.0200	4.00	97.159	95.238
20(C)	6.50	5.0	0.0200	17.0	90.545	84.980
21	6.50	5.0	0.0200	30.0	84.120	94.495
22	4.25	3.5	0.0125	10.5	81.976	90.384
23(C)	6.50	5.0	0.0200	17.0	90.545	90.944
24	8.75	6.5	0.0275	23.5	94.525	97.413
25	4.25	6.5	0.0275	10.5	95.348	90.909
26	4.25	3.5	0.0125	23.5	64.102	60.240
27	4.25	6.5	0.0125	10.5	79.6511	79.084
28(C)	6.50	5.0	0.0200	17.0	85.144	85.433
29(C)	6.50	5.0	0.0200	17.0	85.144	88.432
30(C)	6.50	5.0	0.0200	17.0	85.144	88.076
31	8.75	6.5	0.0275	10.5	94.827	90.797

Table 4.Wave numbers (cm^{-1}) of the vibrational modes of ligand

ligand	$\nu_{\text{C=N}}$ Imine	$\nu_{\text{C=N}}$ Imine	$\nu_{\text{C-N}}$, $\nu_{\text{C-N}}$ aromatic
M	2941.17	1628.18	1595.39, 1552.48, 1417.97
SCH-4	2925.95	1625.28	1586.23, 1482.09, 1417.00

Table 5: Analysis of variance (ANOVA)

Source of variation	M					SCH-4				
	Sum of square	Df ^a	Mean square	F-value	P-value	Sum of square	Df ^a	Mean square	F-value	P-value
X ₁	127.729	1	127.729	17.9149	0.005484	88.295	1	88.295	12.9980	0.011295
X ₁ ²	500.791	1	500.791	70.2394	0.000157	249.621	1	249.621	36.7469	0.000914
X ₂	2.319	1	2.319	0.3253	0.589131	114.514	1	114.514	16.8577	0.006316
X ₂ ²	8.404	1	8.404	1.1787	0.319299	68.180	1	68.180	10.0368	0.019366
X ₃	3565.419	1	3565.419	500.0748	0.000001	1785.555	1	1785.555	262.8525	0.000004
X ₃ ²	462.131	1	462.131	64.8171	0.000196	171.012	1	171.012	25.1747	0.002410
X ₄	511.799	1	511.799	71.7833	0.000148	45.679	1	45.679	6.7245	0.041037
X ₄ ²	10.297	1	10.297	1.4443	0.274728	53.054	1	53.054	7.8101	0.031384
X ₁ X ₂	1.491	1	1.491	0.2092	0.663497	11.573	1	11.573	1.7037	0.239624
X ₁ X ₃	147.147	1	147.147	20.6383	0.003921	25.270	1	25.270	3.7200	0.102025
X ₁ X ₄	0.423	1	0.423	0.0593	0.815772	164.866	1	164.866	24.2701	0.002640
X ₂ X ₃	0.769	1	0.769	0.1079	0.753718	0.055	1	0.055	0.0081	0.931297
X ₂ X ₄	3.634	1	3.634	0.5097	0.502087	366.998	1	366.998	54.0260	0.000325
X ₃ X ₄	184.878	1	184.878	25.9304	0.002239	50.325	1	50.325	7.4084	0.034559
Lack-of-Fit	101.970	10	10.197	1.4302	0.342826	263.462	10	26.346	3.8784	0.055384
Pure Error	42.779	6	7.130			40.758	6	6.793		
Total	5660.113	30				3483.314	30			

^a Degree of freedom

Table 6: Various isotherm constants and correlation coefficients calculated for the adsorption of the Europhtal dye onto Ligands.

Isotherm	Equation	Plot	Parameters	M	SCH-4
				0.03 g	0.02 g
Langmuir	$C_e/q_e = 1/K_a Q_m + C_e/Q_m$	A plot C_e/q_e versus C_e should indicate a straight line of slope $1/Q_m$ and an intercept of $1/(K_a Q_m)$.	Q_{max} ($mg \cdot g^{-1}$)	56.69	17.84
			K_a ($L \cdot mg^{-1}$)	6.563	19.33
			R^2	0.983	0.978
Freundlich	$\ln q_e = \ln K_F + (1/n) \ln C_e$	The values of K_F and $1/n$ were determined from the intercept and slope of linear plot of $\ln q_e$ versus $\ln C_e$, respectively.	$1/n$	0.283	0.339
			K_F ($L \cdot mg^{-1}$)	4.539	3.217
			R^2	0.992	0.994
Temkin	$q_e = B_1 \ln K_T + B_1 \ln C_e$	Values of B_1 and K_T were calculated from the plot of q_e against $\ln C_e$.	B_1	7.019	3.244
			K_T ($L \cdot mg^{-1}$)	184.32	87.28
			R^2	0.918	0.971
Dubinin-Radushkevich	$\ln q_e = \ln Q_s - K \epsilon^2$	Values of Q_m and B were calculated from the plot of ϵ^2 against $\ln q_e$.	Q_s ($mg \cdot g^{-1}$)	38.63	14.48
			$B \times 10^{-8}$	1.10	1.70
			E	6742	5423
			R^2	0.797	0.933

Table 7: Kinetic parameters for the adsorption of the Europhtal dye onto Ligands.

Model	Equation	plot	Parameters	Value of parameters	
				M	SCH-4
				5 mg L ⁻¹	40 mg L ⁻¹
First-order kinetic	$\log(q_e - q_t) = \log q_e - \left(\frac{k_1}{2.303}\right)t$	Plot the values of $\log(q_e - q_t)$ versus t to give a linear relationship from which k_1 and q_e can be determined from the slope and intercept, respectively.	k_1 (min ⁻¹)	0.087	0.126
			q_e (calc) (mg g ⁻¹)	1.060	1.373
			R^2	0.914	0.874
Pseudo-second-order kinetic	$\frac{t}{q_t} = \frac{1}{k_2 q_e^2} + \frac{t}{q_e}$	Plot the values of (t/q_t) versus t to give a linear relationship from which k_2 and q_e can be determined from the slope and intercept, respectively.	k_2 (min ⁻¹)	0.005	0.149
			q_e (calc) (mg g ⁻¹)	6.20	33.45
			R^2	0.999	0.999
Intraparticle diffusion	$q_t = K_{\text{dif}} t^{1/2} + C$	The values of K_{dif} and C were calculated from the slopes of q_t versus $t^{1/2}$.	K_{dif} (mg g ⁻¹ min ^{-1/2})	0.226	0.715
			C (mg g ⁻¹)	4.790	30.163
			R^2	0.972	0.920
Elovich	$q_t = \frac{1}{\beta} \ln(\alpha\beta) + \frac{1}{\beta} \ln t$	Plot the values of (q_t) versus $\ln(t)$ to give a linear relationship from which α and β can be determined from the slope and intercept, respectively.	β (g mg ⁻¹)	2.477	1.1756
			α (mg g ⁻¹ min ⁻¹)	99.89	35.842
			R^2	0.940	0.960
			q_e (exp) (mg g ⁻¹)	5.989	33.139

Table 8.

Percentage removal of the Europhtal dye from four different effluents (N=3).

Samples	Initial dye concentration (mg L ⁻¹)	Removal (%)	
		M-AC	SCH-4-AC
River water	30	99.50±1.4	99.21±0.7
Sanitary wastewater	30	98.75±2.5	99.12±1.21
Industrial waste	30	97.54±1.9	96.63±2.5
Water output from the refinery	30	97.62±2.1	96.45±1.7

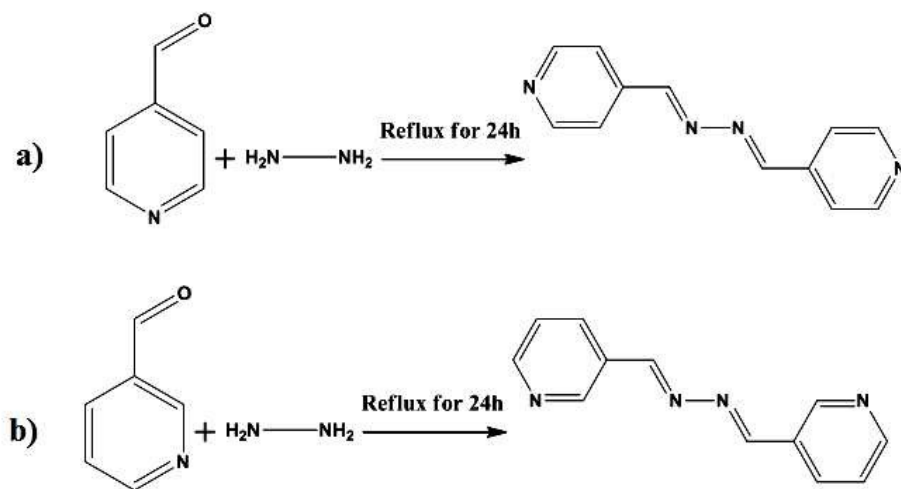


Fig. 1

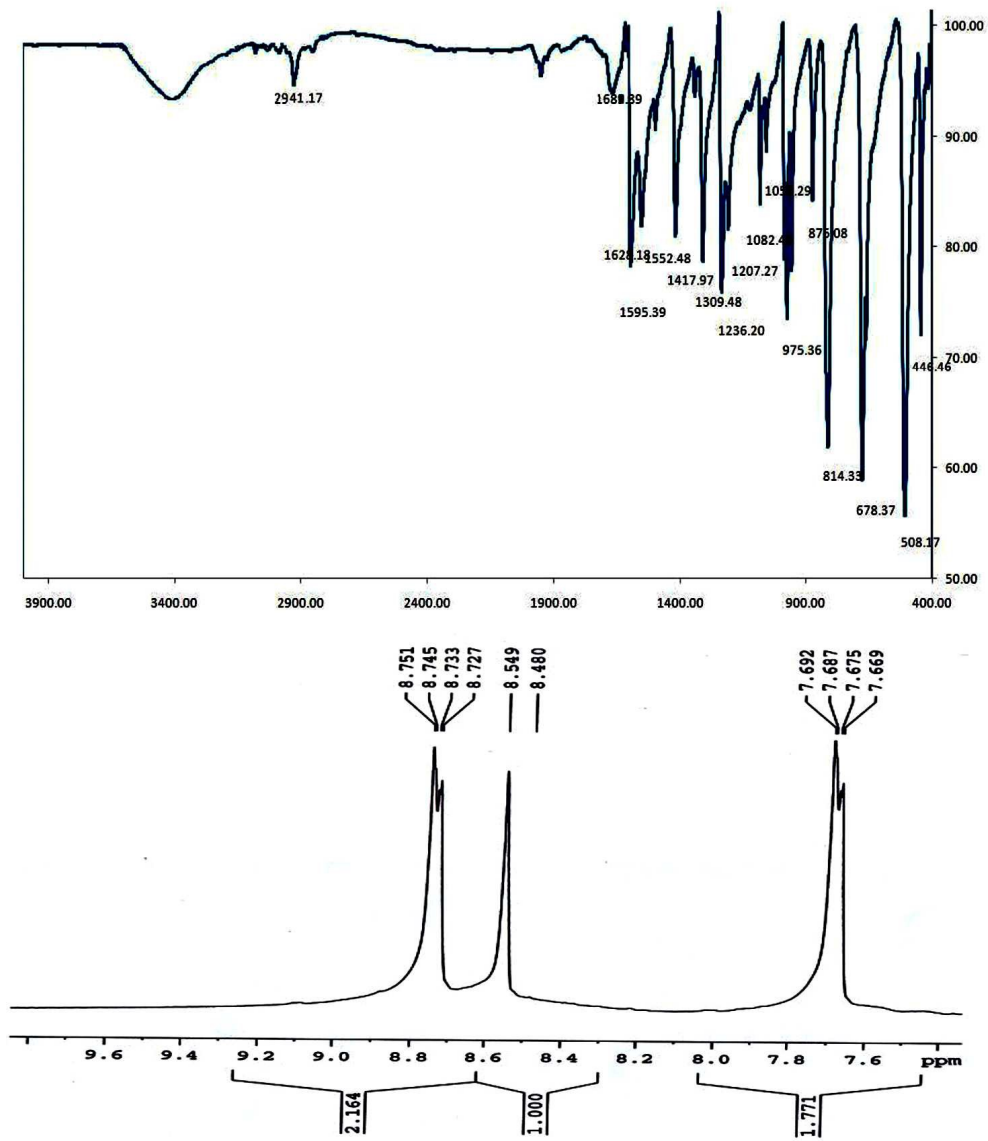


Fig. 2

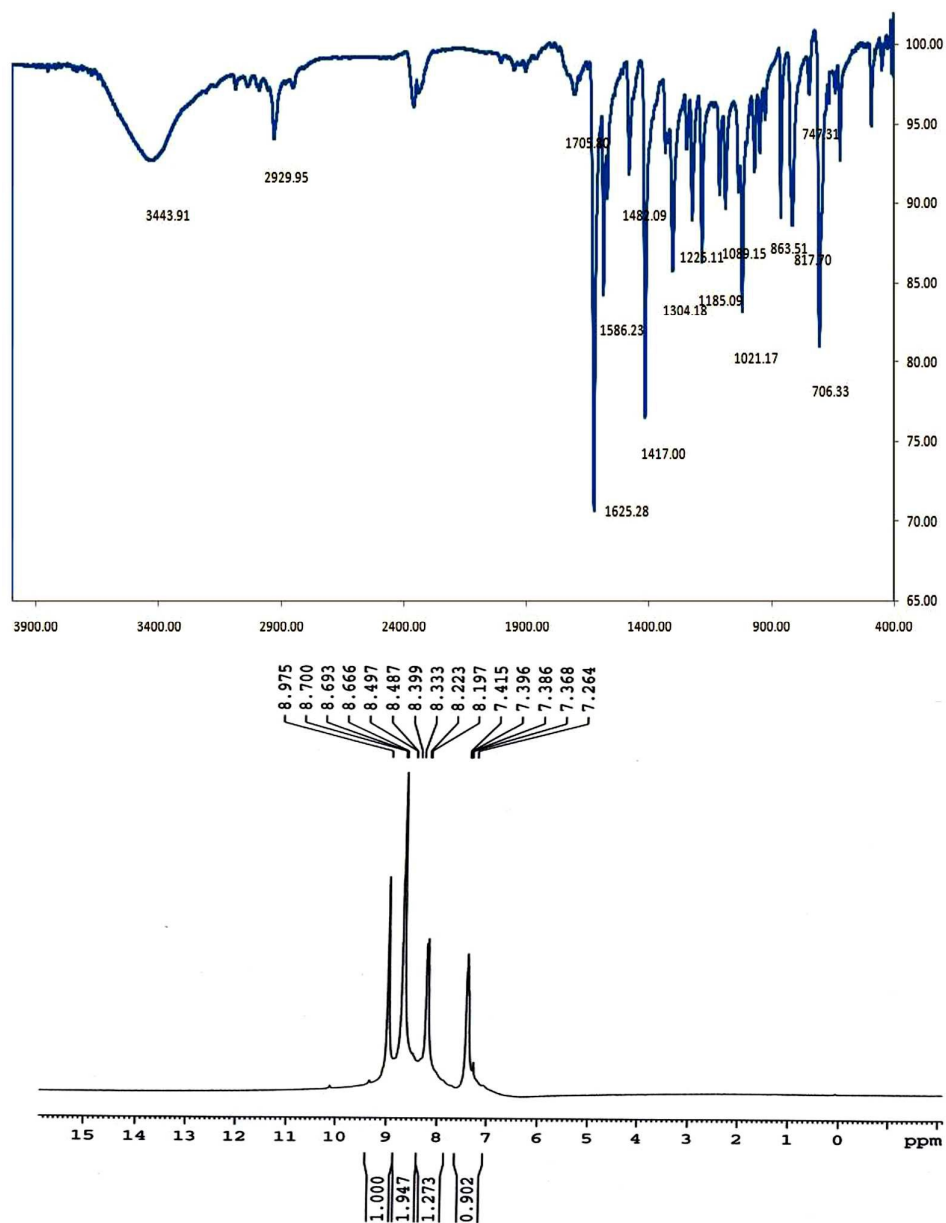


Fig. 3

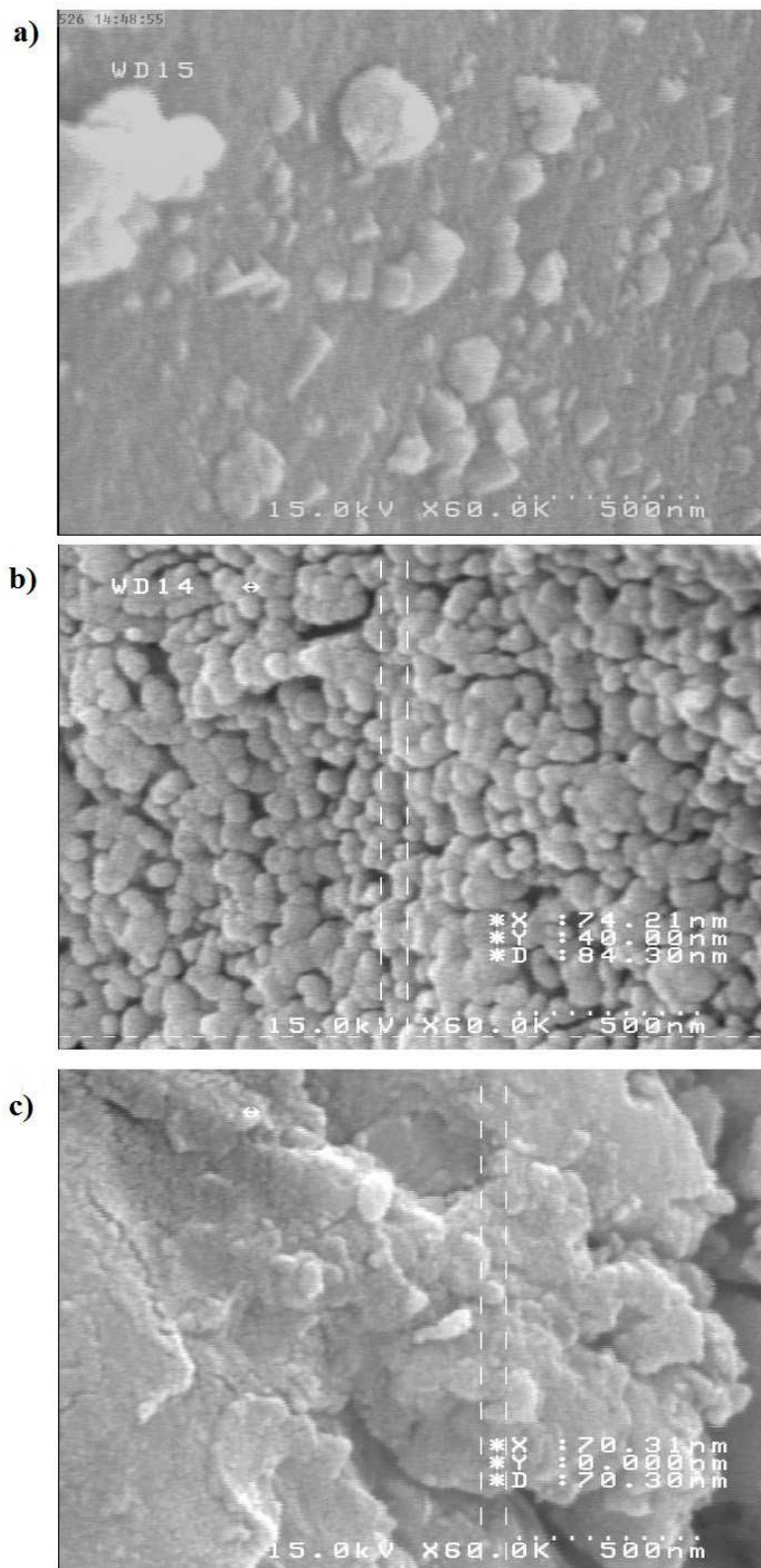


Fig.4

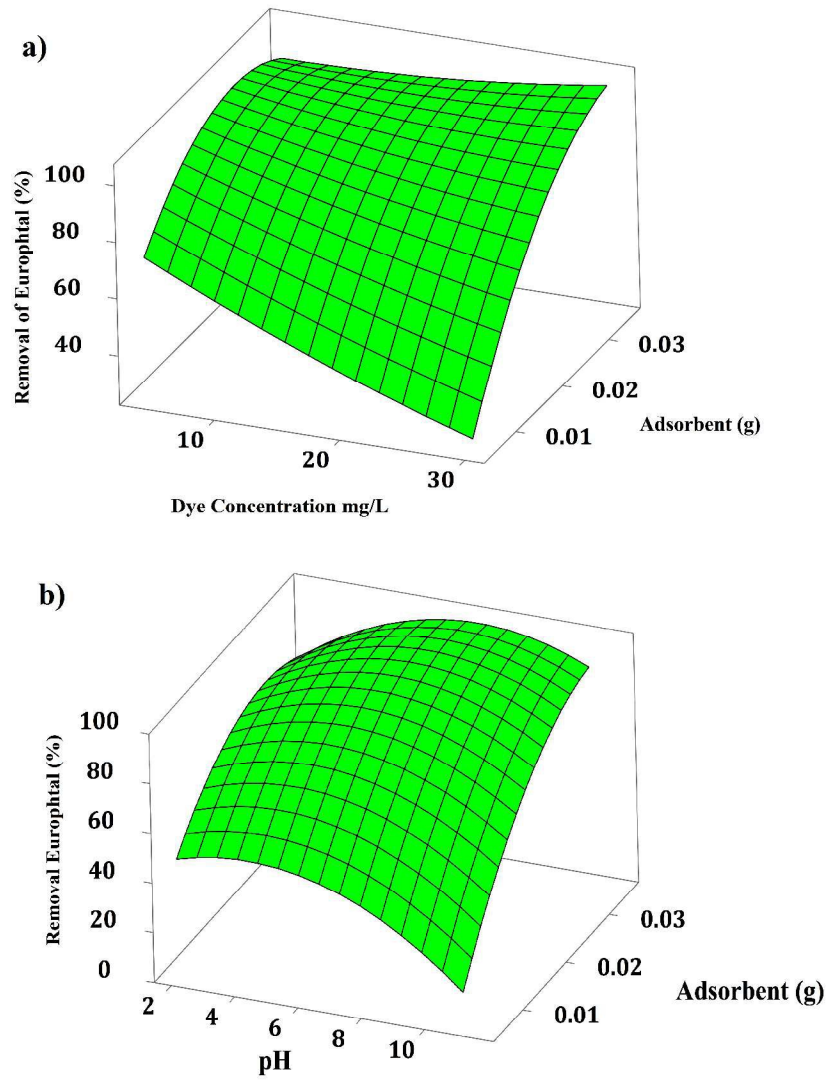
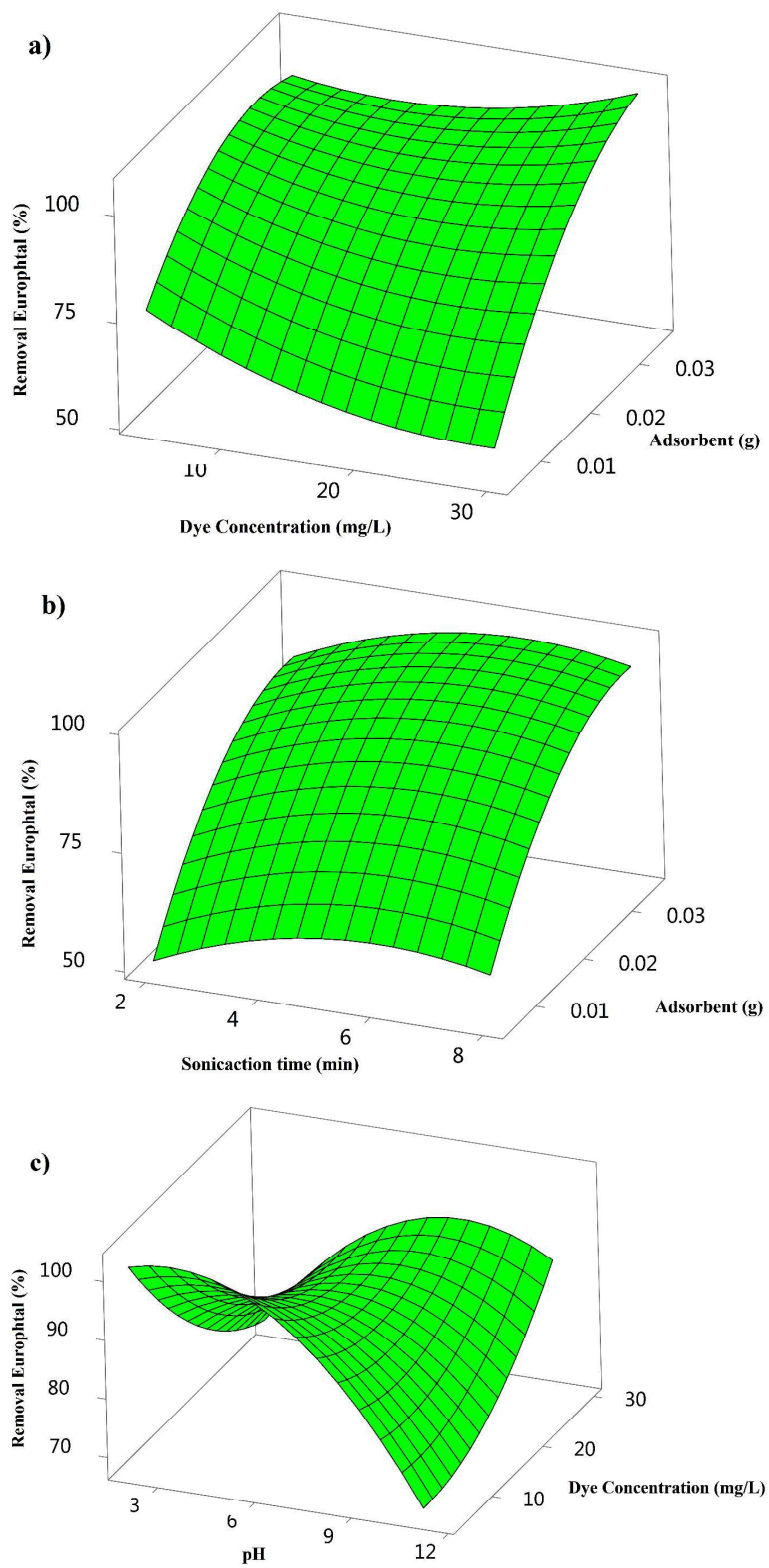


Fig. 5

**Fig. 6**

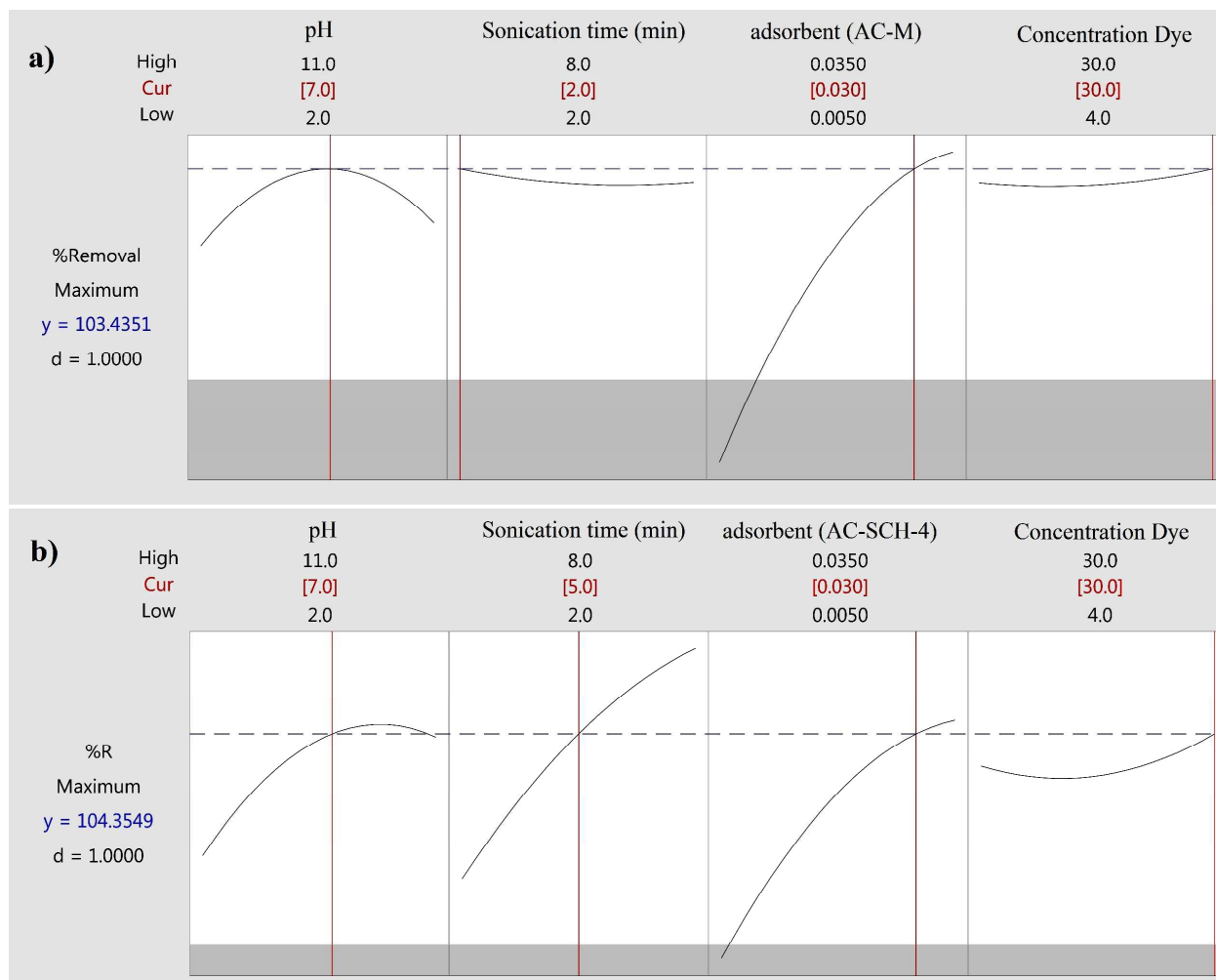


Fig. 7

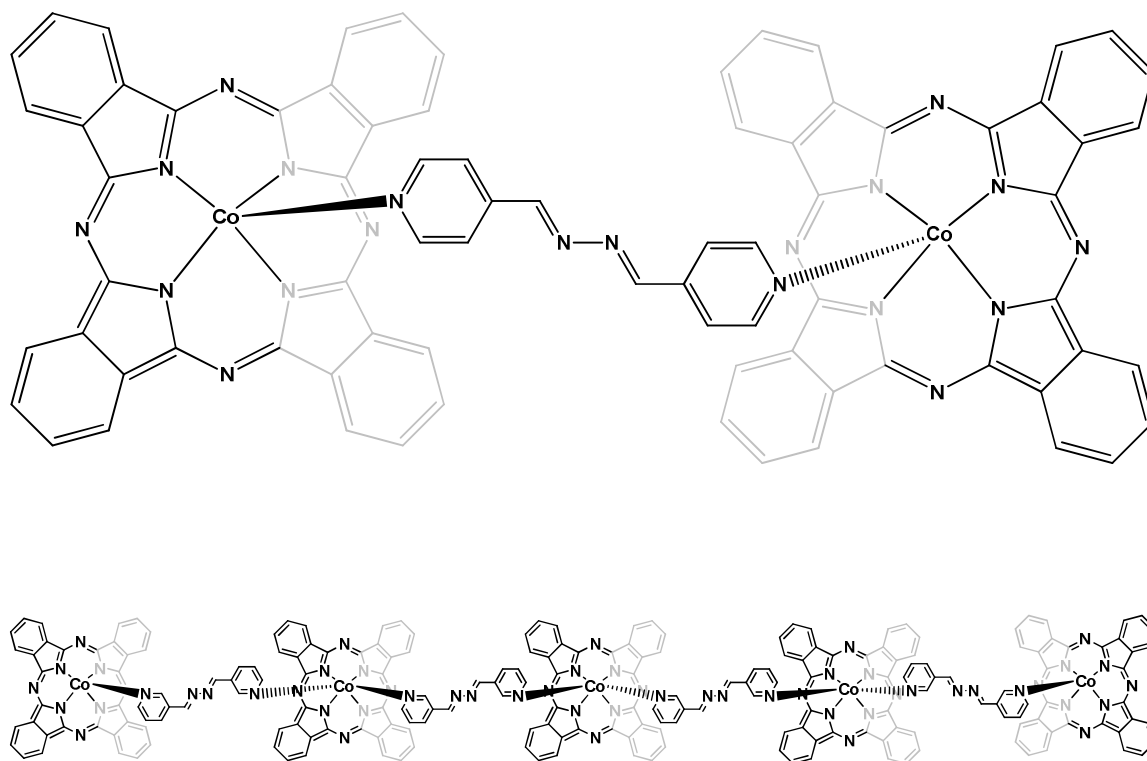


Fig. 8.

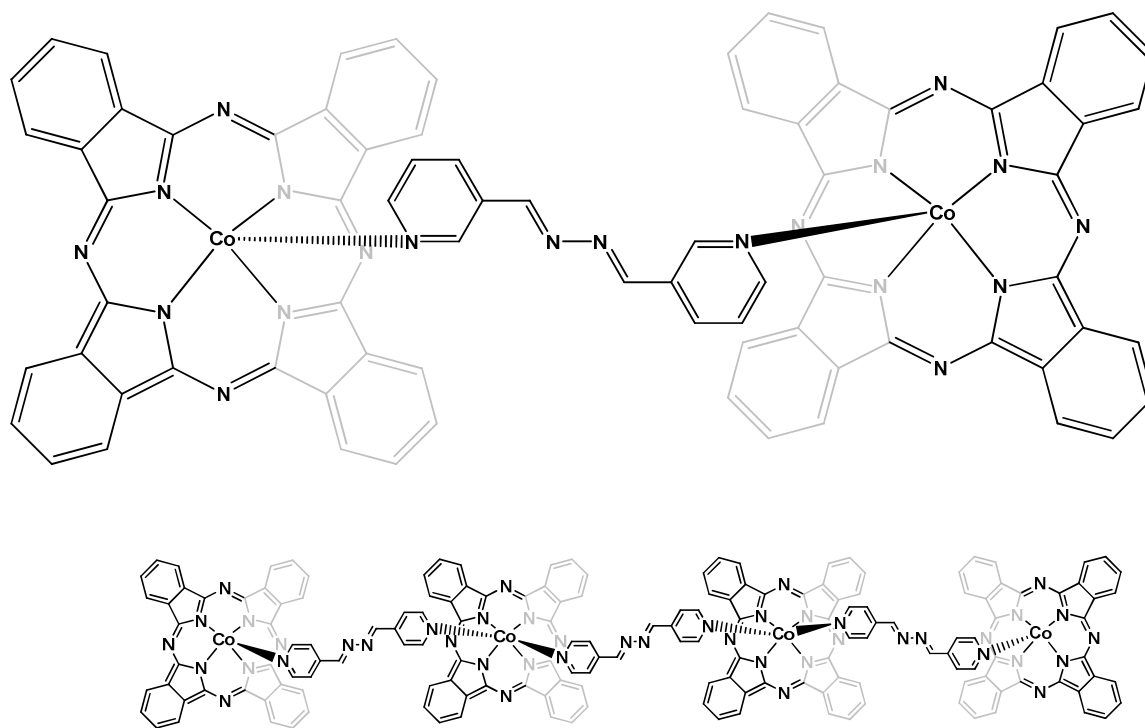


Fig. 9.